



Electrochemically deposited poly(3,4-propylenedioxythiophene) for dye-sensitized solar cell

Samia Belhousse¹ · Fatma-Zohra Tighilt¹ · Khaled Hamdani¹ · Ibtissam Aouali² · Samir Benouart² · Naima Belhaneche² · Kahina Lasmi¹ · Amar Manseri¹ · Sabrina Sam¹

Received: 28 October 2021 / Accepted: 1 January 2022 / Published online: 7 January 2022
© The Author(s), under exclusive licence to Springer Nature B.V. 2022

Abstract

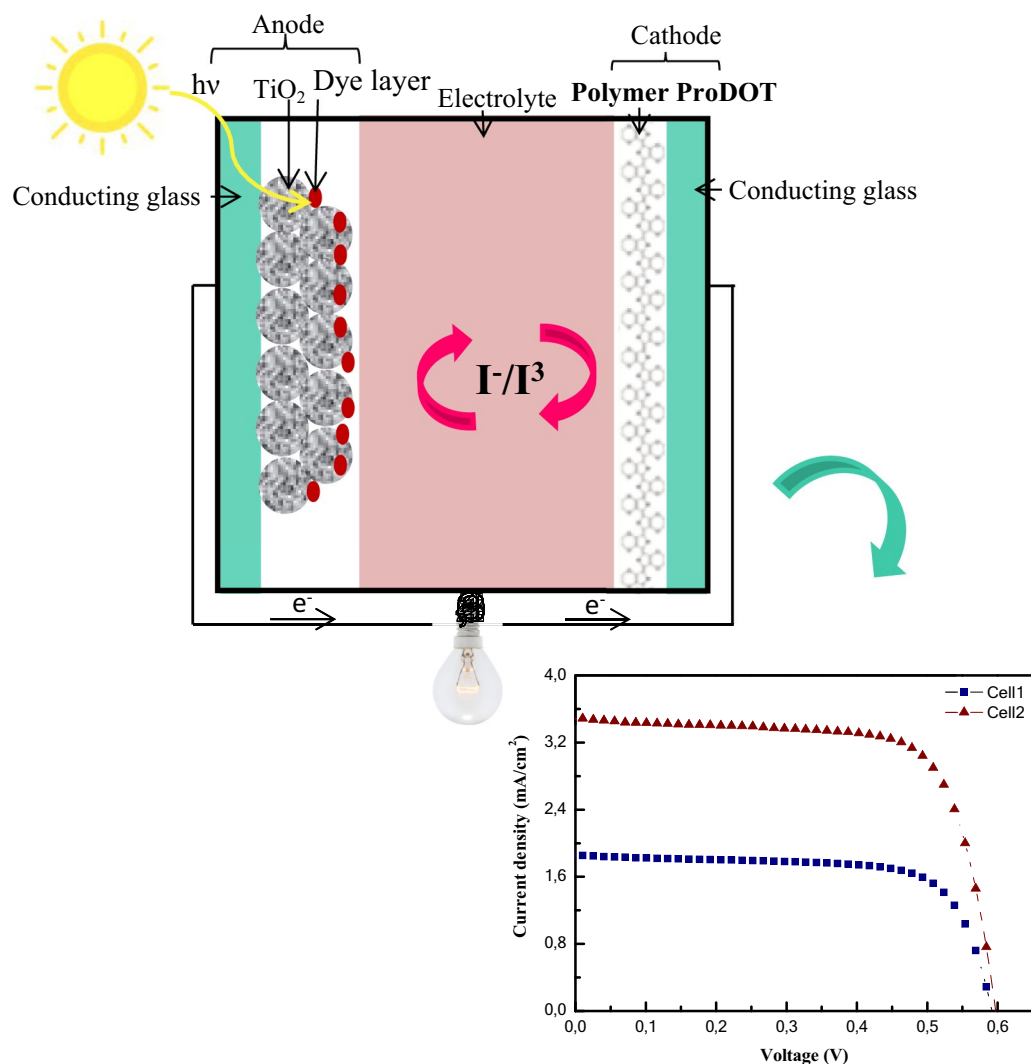
In this work, poly(3,4-propylenedioxythiophene) (PProDOT)-based counter electrode (CE) was elaborated. The PProDOT polymer was electropolymerized by using chronoamperometry on fluorine-doped tin oxide glass substrates in acetonitrile and tetrabutylammonium perchlorate-based solution containing 3,4-propylenedioxythiophene (ProDOT) monomer. The thickness of PProDOT CE was controlled by the polymerization time. The effect of applied time on the surface morphology was studied by scanning electron microscopy. Fourier transform infrared spectroscopy in ATR mode and contact angle measurements was used to investigate the polymer films, as well. The electrocatalytic activity of PProDOT CEs was studied in I^-/I_3^- electrolyte.

✉ Samia Belhousse
Belhoussesamia@crtse.dz

¹ Division Couches Minces Surfaces Interfaces (CMSI),
Centre de Recherche en Technologie des Semi-Conducteurs
Pour L'Energétique (CRTSE), 2 Bd. Frantz Fanon, B.P. 140,
Alger-7 merveilles, Algiers, Algeria

² Ecole Nationale Polytechnique (ENP), 10, Avenue Hassen
Badi, B.P. 182, El Harrach, 16200 Algiers, Algeria

Graphical abstract



Keywords Poly(3,4-propylenedioxythiophene) · Electropolymerization · Counter electrode · Dye-sensitized solar cell

1 Introduction

Since the most recent decades, dye-sensitized solar cells (DSSCs) have been attracting considerable attention because of high theoretical efficiency, simple fabrication process, low fabrication cost, and good flexibility [1, 2]. A standard DSSC consists of a porous nanocrystalline TiO₂ photoanode sensitized by a dye to absorb visible light, an iodide/tri-iodide redox electrolyte and a counter electrode (CE).

CE is an important component of DSSCs having a significant influence on performance, long-term stability and cost of the devices. As positive electrode, CE collects

electrons from the external circuit and enables efficient charge transfer at the electrode/electrolyte interface. Moreover, CE undertakes the function of catalyst for the reduction reaction of I³⁻ to I⁻ promoting thus the generation of the electrolyte. A typical DSSC counter electrode was made by platinum (Pt) metal because of its excellent catalytic activity and high conductivity. However, Pt is an expensive metal [3] and the fabrication of Pt CE needs heat treatment and it is unfavorable for the development of flexible plastic substrate, thus limits its practical application [4]. Therefore, it is necessary to explore alternative Pt-free materials with good electroconductivity and electrocatalytic activity toward the reduction of tri-iodide ions, with cheaper price to reduce the cost of DSSCs.

Many efforts have been devoted over the past few years to explore alternatives to substitute the expensive Pt catalyst, such as inorganic semiconductor [5, 6], carbonaceous materials [7–10], conducting polymers [11–15], and hybrid materials [16, 17].

Conjugated polymers having advantages including low cost, ease of fabrication, flexibility, and potential of large area production [18] possess a promising role in the especially application of organic solar cells. Microporous polyaniline as counter electrode has shown an efficiency of 7.1% in DSSCs [14], whereas PANI is not the material of choice due to its instability and self-oxidation properties. Polythiophene derivatives are known for their high conductivity, electrochemical stability, and high catalytic activity [19]. Among these derivatives, alkyl polythiophenes are insoluble material and can be polymerized by electrochemical way, allowing thin layers of p-conjugated polymers to be easily coated on any conducting and flexible substrate under ambient conditions with low cost. In particular, poly(3,4-propylenedioxythiophene) (PProDOT) is suitable to be utilized as a CE due to its good stability, high electrochemical activity, and excellent transparency.

Herein, we report on the growth of PProDOT using Chronoamperometry technique on FTO substrate as CEs for DSSCs. The electrocatalytic activity of these CEs toward I_3^- reduction was studied. The effect of deposition time on the surface morphology of these CEs and on the photovoltaic performances of the DSSCs was investigated, as well.

2 Experimental

2.1 Preparation of electropolymerized PProDOT CE

Chronoamperometry technique was used to achieve the electropolymerization of ProDOT monomer (97% Aldrich) on FTO substrate. The applied potential is 2.8 V vs. Ag/AgCl for 1 and 2 s with a sweep rate of 50 mV s⁻¹ using Autolab potentiostat controlled by Nova software-equipped computer. The value of the applied potential was chosen from the cyclic voltammograms recorded in 0.05 M ProDOT monomer on FTO in 0.1 M tetrabutylammonium perchlorate (TBAP) ≥ 99% (Aldrich). Prior to electropolymerization, FTO transparent glasses (Aldrich) were pretreated using an ultrasonic bath in detergent, deionized water, acetone (Aldrich), and ethanol (Aldrich) for 10 min, respectively. Then the electropolymerization of ProDOT was carried out using the cleaned FTO substrate as a working electrode, Au electrode as counter electrode, and a saturated Ag/AgCl reference electrode in an aqueous solution containing 0.05 M of ProDOT monomer and 0.1 M TBAP. After the electropolymerization, the obtained PProDOT CE surfaces were rinsed in acetonitrile and in deionized water and dried with N₂ stream.

2.2 Characterization of PProDOT CEs

The obtained structures were analyzed by FTIR-ATR spectroscopy with Alpha Bruker spectrometer equipped with diamond crystal. All FTIR spectra were collected with 64 scans in mid infrared region at 2 cm⁻¹ resolution. The surface morphologies of electropolymerized PProDOT were studied using scanning electron microscopy (SEM, Joel JSM-7610FPlus) and contact angle measurements were performed by means of a remote computer-controlled goniometer system (DIGIDROP), using deionized water. All measurements were made in ambient atmosphere at room temperature. The polymer was also characterized by cyclic voltammetry (CV) in 0.1 M TBAP using Autolab potentiostat. To evaluate the electrocatalytic activity of CEs, CV was carried out using the aforementioned electrochemical analyzer. The CVs were performed using Au wire as counter electrode, Ag/AgCl as reference electrode, and PProDOT/FTO as working electrode in acetonitrile solution consisting of 50 mM LiI, 10 mM I₂, and 500 mM LiClO₄. The data were acquired in the potential interval ranging from -2 to 3.5 V.

2.3 Fabrication of DSSCs

The photoanode was prepared using synthesized TiO₂ nanoparticles as described previously [20]. TiO₂ paste was deposited on the FTO substrate using Doctor Blade technique. The electrode was soaked in 0.3 mM ethanolic solution of N719 dye for 24 h, and then washed with ethanol, and dried with a nitrogen flow. The dye-sensitized TiO₂ electrode and PProDOT counter electrode were assembled into the sealed sandwich-type cells by heating with a hot-melt film used as spacers between the electrodes. The electrolyte solution is composed of 0.1 M LiI, 0.05 M I₂, 0.6 M 1,2-dimethyl-3-propylimidazolium iodide (DMPII), and 0.5 M tert-butyl pyridine with acetonitrile as the solvent. Current–voltage characteristics J(V) of the DSSCs were performed by using potentiostat/galvanostat (Metrohm Autolab). Light intensity was adjusted at simulated AM 1.5G illumination condition (100 mWcm⁻²).

3 Results and discussion

3.1 PProDOT electropolymerization

Prior to the electropolymerization of PProDOT by chronoamperometry technique, CVs were performed in ProDOT monomer solution in order to study the electrochemical behavior of the monomer and determine its oxidation potential. Figure 1 shows the cyclovoltametric curves of 0.05 M ProDOT in acetonitrile solution containing 0.1 M

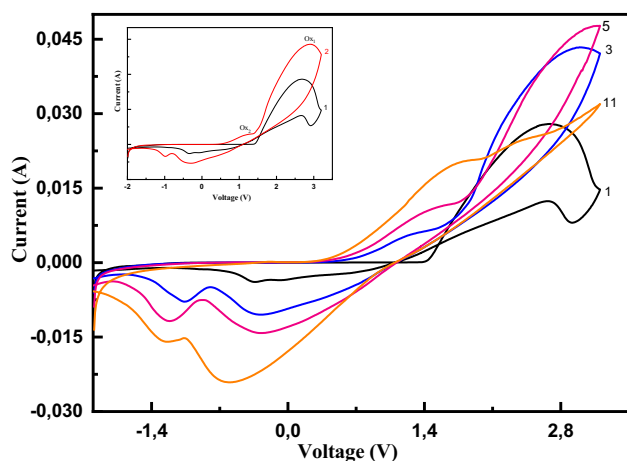


Fig. 1 Cyclic voltammograms of acetonitrile solution containing 0.05 M ProDOT and 0.1 M TBAP, $v = 50 \text{ mV/s}$

TBAP, achieved on FTO surface, at a potential range from -2 to 3 V under potential sweep rates of 50 mV s^{-1} .

During the first scanning, we observe the appearance of an oxidation peak around 2.6 V which corresponds to the maximum oxidation of ProDOT to radical cation. On the return, we notice a reduction peak around -0.36 V assigned to the reduction of the polymer or the oligomer formed on FTO surface. During the second scanning cycle, two oxidation peaks labeled Ox_1 and Ox_2 are observed. Ox_1 peak corresponding to the monomer oxidation is slightly shifted to 2.90 V due to the changes occurred on the surface after the first cycle passage. Ox_2 peak appears around 1.29 V and corresponds to the oxidation of ProDOT oligomer formed on FTO surface. The intensity of this oxidation peak increases with the number of sweeps indicating the evolution of the polymer chains. After the first reverse scan, two reduction peaks were appeared, Red_1 around -1 V and Red_2 around -0.33 V . The two peaks correspond to the reduction of the monomer and the formed polymer, respectively. As the number of scans increases, the reduction peaks Red_1 and Red_2 shift to more negative values and reach -0.61 V and -1.27 V , respectively. This clearly means that the values of the oxidation and the reduction of the polymer depend on surface state.

According to the CV results, we applied 2.8 V during PProDOT electropolymerization by chronoamperometry in acetonitrile solution containing 0.05 M ProDOT and 0.1 M TBAP. It is well known that chronoamperometry method is more suitable for a better control of polymer thickness. In this study, we applied two durations 1 s and 2 s . Figure 2 depicts the chronoamperometric curve of 2 s deposition. At the beginning of polymerization process, the current increases drastically from 0.073 A to reach in

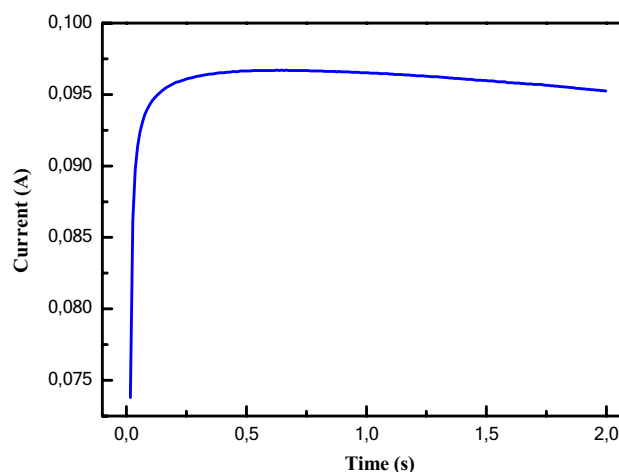


Fig. 2 Chronoamperometry curve of the electropolymerization of PProDOT for 2 s in acetonitrile solution containing 0.05 M ProDOT and 0.1 M TBAP

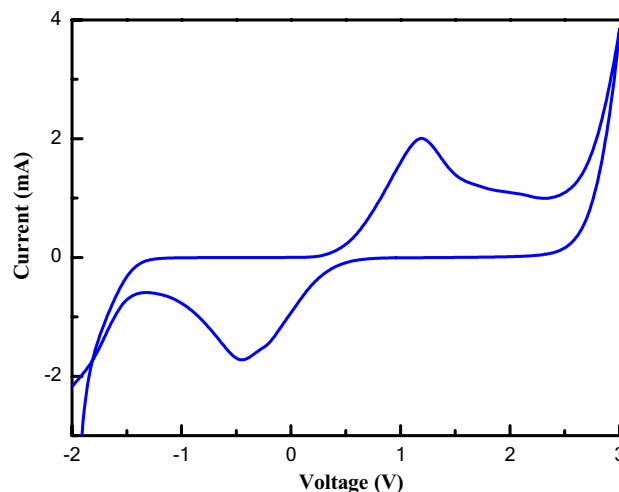


Fig. 3 Electrochemical characterization of electropolymerized PProDOT in 0.1 M TBAP acetonitrile solution, $v = 50 \text{ mV/s}$

tenth of a second a steady value of 0.097 A corresponding to polymerization current.

3.2 Electrochemical characterization of electropolymerized PProDOT

The electrochemical behavior of electropolymerized PProDOT was studied by CV in monomer-free acetonitrile electrolytic solution containing 0.1 M TBAP. Figure 3 displays the electrochemical response of PProDOT to a potential sweep between 2 and 3 V showing up the polymer redox process with an oxidation peak around 1.2 V and a reduction peak around -0.44 V . These values corroborate with those found in the previous section.

Fig. 4 ATR-FTIR spectrum of electropolymerized PProDOT on FTO

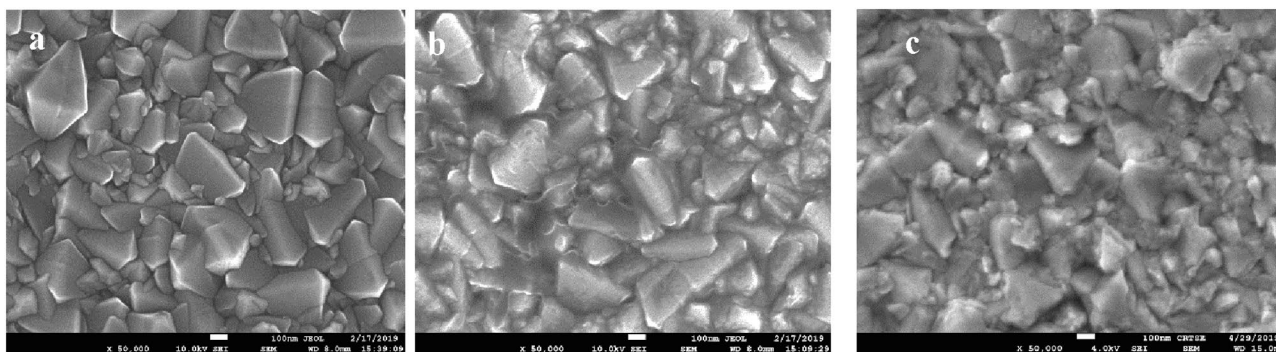
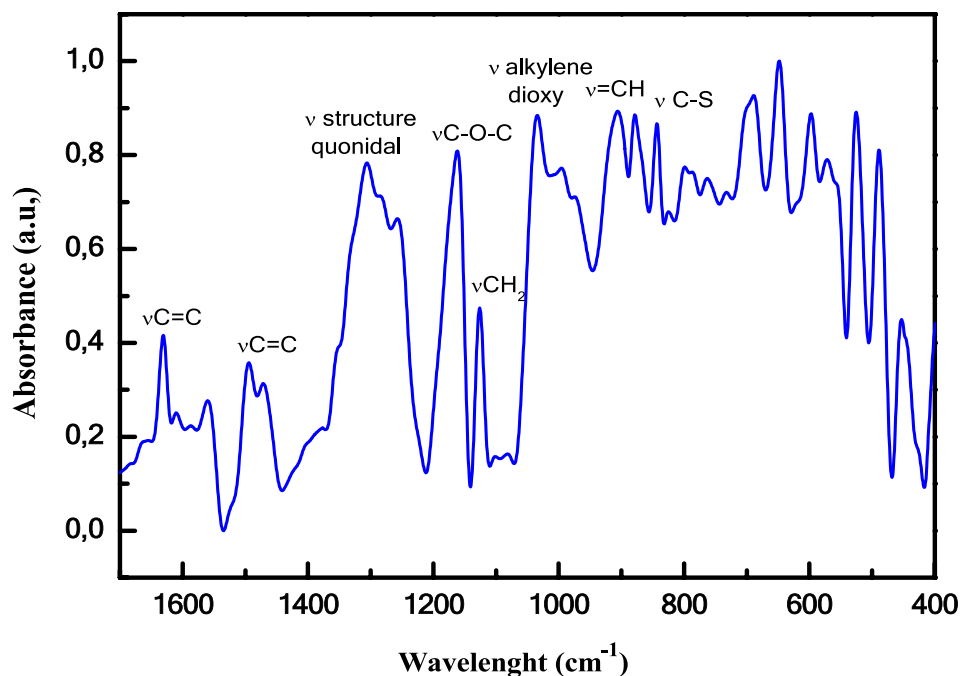


Fig. 5 SEM images of electropolymerized PProDOT on FTO at different polymerization times. **a** FTO, **b** 1 s, **c** 2 s

3.3 ATR-FTIR characterization

The ATR-FTIR spectrum of electropolymerized PProDOT surface is depicted in Fig. 4. All the bands assignment confirms the polymerization of PProDOT on the FTO surface. Indeed, we observe a band at 1631 cm^{-1} which corresponds to the stretching vibration of C=C double bond [21] and the bending mode of this bond is also presented by a band around 1490 cm^{-1} [21, 22].

The band at 1276 cm^{-1} is assigned to the bending vibrations of the quonidal structure [22]. The stretching vibration of C–O bond is represented by the 1159 cm^{-1} [22] band while the 1121 cm^{-1} band is attributed to the stretching vibration of C–S bond [21]. The corresponding bending mode of C–S bond appears around 872 cm^{-1} [22].

3.4 SEM observations

The evolution of FTO surface morphology before and after PProDOT electropolymerization for two deposition times is illustrated in Fig. 5. The naked FTO surface displays a regular structure with geometrical shapes (Fig. 5a). After PProDOT electrodeposition for 1 s, the FTO basic structure remains apparent (Fig. 5b) indicating that the electropolymerized PProDOT for 1 s is very thin and transparent. As the deposition time increases to 2 s, the polymer grows further and the layer becomes thicker (Fig. 5c).

3.5 Contact angle measurements

Contact angle measurements performed on FTO surface before and after PProDOT electropolymerization (Fig. 6)

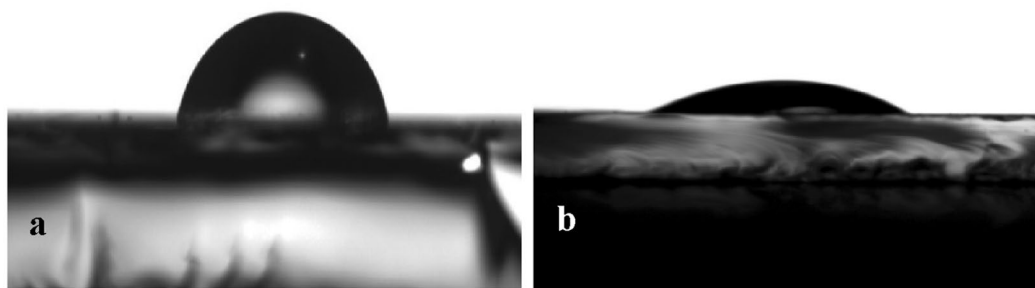
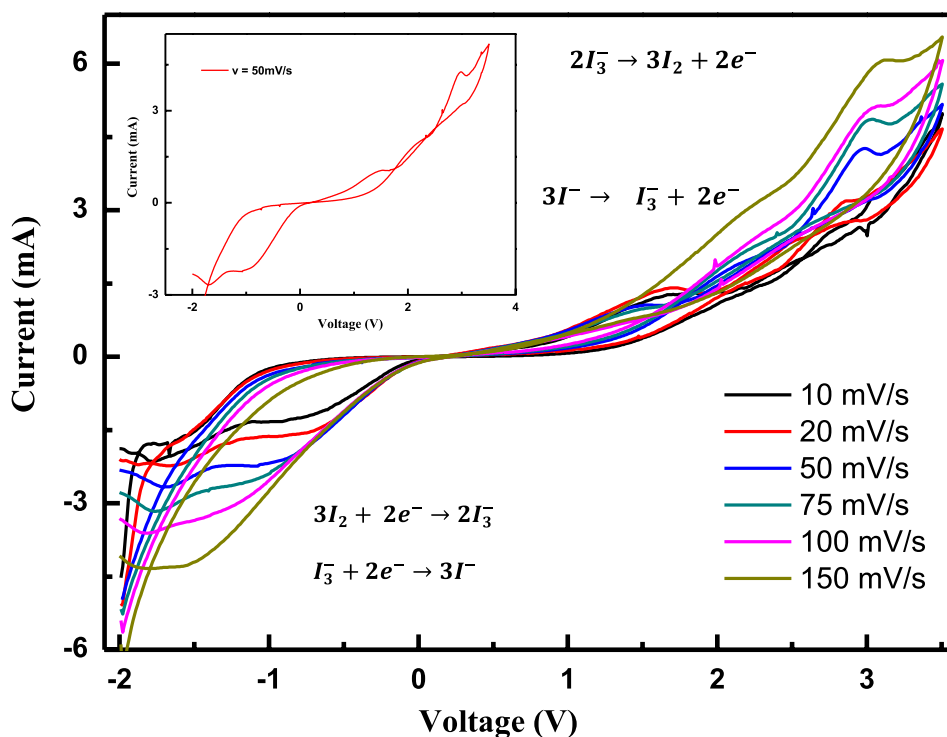


Fig. 6 Contact angle measurements performed on FTO surface. **a** Before and **b** after PProDOT electropolymerization

Fig. 7 Cyclic voltammetry of iodide species on electropolymerized PProDOT surface in an acetonitrile solution with 50 mM LiI, 10 mM I_2 , and 500 mM $LiClO_4$

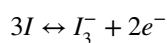


confirm the chemical changes occurred on the surface. The clean FTO surface exhibits an average contact angle of 77° (Fig. 6a). When the FTO surface is covered with the electropolymerized PProDOT, the value of the contact angle decreases to 36° which is representative of the hydrophilic nature of the electrodeposited polymer (Fig. 6b). This characteristic would be beneficial for the operation of the CE.

3.6 Electrocatalytic activity

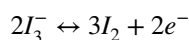
The regeneration of redox species I^-/I_3^- is made through the reduction of I_3^- on the CEs of DSSCs. To study the electrocatalytic activity of CEs toward I_3^- reduction, CV experiments were conducted at several scan rates in acetonitrile

solution containing 50 mM LiI, 10 mM I_2 , and 500 mM $LiClO_4$. Two pairs of redox peaks were observed in the CV measurements (Fig. 7). The more cathodic redox pair corresponds to the following reaction [23]:



The observation of I^-/I_3^- redox couple indicates the efficiency of electropolymerized PProDOT CE toward the reduction of I_3^- ,

whereas the more anodic pair represents the redox reaction of I_2 [24]:



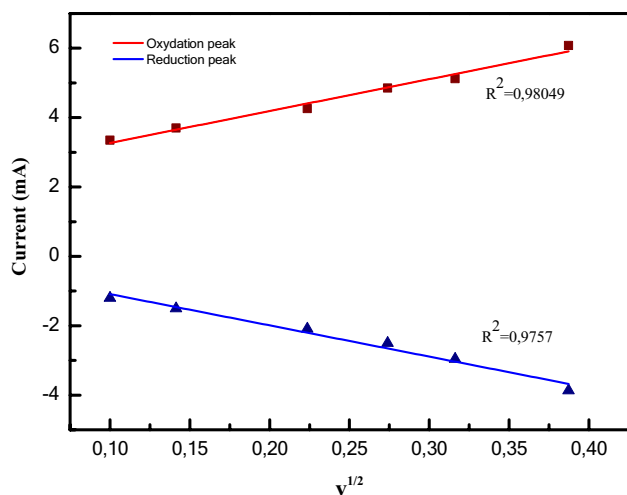


Fig. 8 Cathodic and anodic peak current as a function of scan rate

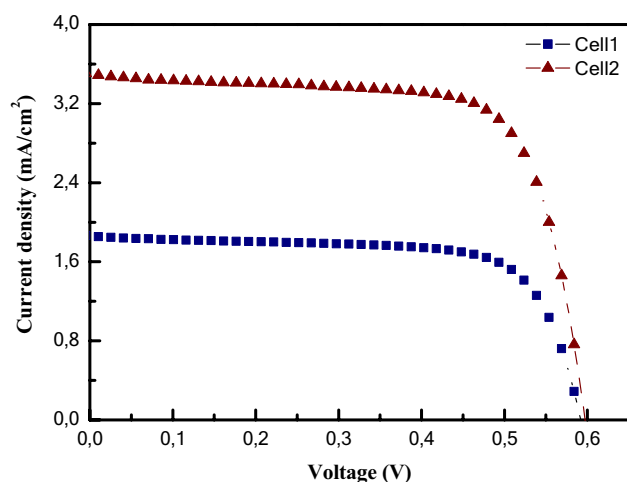


Fig. 9 Current–voltage curves of the DSSCs

This reaction is unimportant for the operation of DSSCs.

Figure 8 shows the plot of the cathodic and anodic peaks intensity as a functions of the square root of the scan rate. The linear relationship indicates that the redox reaction at the PProDOT surface is an electrochemical process controlled by species diffusion, i.e., occurred in solution. This also suggests that no specific interaction between I^-/I_3^- and the PProDOT electrode occurred as is the case of platinum electrode [12].

3.7 Photovoltaic measurements

Two types of DSSCs labeled Cell1 and Cell2 have been studied and correspond to the cells made with 1 s and 2 s electropolymerized PProDOT CE, respectively. Figure 9 shows

Table 1 Photovoltaic performances of the DSSCs

Cell	J_{sc} (mAcm ⁻²)	V_{oc} (V)	P_{max} (mW)	FF ^a (%)	η^b (%)
1	1.860	0.590	0.198	0.720	0.79
2	3.496	0.597	0.374	0.716	1.50

$$^a\text{FF} = P_{\text{max}} / (I_{\text{sc}} \times V_{\text{oc}}) \times 100$$

$$^b\eta (\%) = I_{\text{sc}} \times V_{\text{oc}} \times \text{FF} / \text{total incident energy} \times 100$$

the current–voltage (J–V) photovoltaic performance curves under AM 1.5 illumination (100 mW cm⁻²) of the DSSCs. The short-circuit photocurrent density (J_{sc}), the open-circuit voltage (V_{oc}), the fill factor (FF), and the energy conversion efficiency (η) of the cells are summarized in Table 1.

We can observe that both Cell1 and Cell2 present high FF (around 0.72%) and V_{oc} of about 0.59 V. However, Cell1 owns lower J_{sc} with a value of 1.860 mA cm⁻² giving an overall efficiency of 0.79%, while J_{sc} of Cell2 increases to 3.456 mA cm⁻² leading to the rising of its efficiency (1.50%), though its V_{oc} and FF remain almost the same compared to Cell1.

As seen in SEM observations, the electropolymerized PProDOT in Cell2 is porous and thicker than in Cell1. This implies a large surface area of the PProDOT film and thus many active sites that could reduce a greater quantity of I_3^- ions which in turn generate larger amount of reduced dye molecules, leading to the higher value of J_{sc} recorded for Cell2.

4 Conclusion

The effects of PProDOT conducting polymer as counter electrode on the performance of platinum-free DSSCs were studied. The CV measurement involving the I^-/I_3^- redox reaction on the electropolymerized PProDOT electrode showed good catalytic property for reducing I_3^- and no specific adsorption of the ions was observed. When comparing the DSSCs based on electropolymerized PProDOT for 1 s and 2 s, this latter displayed the best conversion efficiency of 1.50% with higher J_{sc} value of 3.456 mA cm⁻²; this was due to the higher surface active area from its porous structure. These results suggested that porous PProDOT CE was effective to improve the photovoltaic performance of DSSCs. However, to compete platinum, some optimizations in terms of structure, thickness, and porosity should be done.

Acknowledgements We acknowledge the National Research Fund (DGRSDT) and the Centre de Recherche en Technologie des Semi-conducteurs pour l’Énergétique (CRTSE).

Funding This research was supported by the National Research Fund of the Directorate-General for Scientific Research and Technological Development (Algeria).

Declarations

Conflict of interest We wish to confirm that there is no known conflict of interests of interest associated with this publication.

References

- Grätzel M (2001) Photoelectrochemical Cells. *Nature* 414:338–344. <https://doi.org/10.1038/35104607>
- Grätzel M (2009) Recent advances in sensitized mesoscopic solar cells. *Acc Chem Res* 42:1788–1798. <https://doi.org/10.1021/ar900141y>
- Zhou H, Shi Y, Qin D, An J, Chu L, WangCh WangY, Guo W, Wang L, Ma T (2013) Printable fabrication of Pt-and- ITO free counter electrodes for completely flexible quasi-solid dye-sensitized solar cells. *J Mater Chem A* 1:3932–3937. <https://doi.org/10.1039/C3TA00960B>
- Smestad G, Bignozzi C, Argazzi R (1994) Testing of dye sensitized TiO₂ solar cells I: experimental photocurrent output and conversion efficiencies. *Sol Energy Mater Sol Cells* 32:259–272. [https://doi.org/10.1016/0927-0248\(94\)90263-1](https://doi.org/10.1016/0927-0248(94)90263-1)
- Wang M, Anghel AM, Bt M, Cevey Ha NL, Pootrakulchote N, Zakeeruddin SM, Grätzel M (2009) CoS supersedes Pt as efficient electrocatalyst for triiodide reduction in dye-sensitized solar cells. *J Am Chem Soc* 131:15976–15977. <https://doi.org/10.1021/ja905970y>
- Wu M, Lin X, Hagfeldt A, Ma T (2011) Low-cost molybdenum carbide and tungsten carbide counter electrodes for dye-sensitized solar cells. *Angew Chem Int* 50:3520–3524. <https://doi.org/10.1002/anie.201006635>
- Sahito IA, Sun KC, Arbab AA, Qadir MB, Choi YS, Jeong SH (2016) Flexible and conductive cotton fabric counter electrode coated with graphene nanosheets for high efficiency dye sensitized solar cell. *J Power Sources* 319:90–98. <https://doi.org/10.1016/j.jpowsour.2016.04.025>
- Calogero G, Calandra P, Sinopoli A, Gucciardi PG (2010) Metal nanoparticles and carbon-based nanostructures as advanced materials for cathode application in dye-sensitized solar cells. *Int J Photoenergy* 2010:1–15. <https://doi.org/10.1155/2010/109495>
- Trancik JE, Barton SC, Hone J (2008) Transparent and catalytic carbon nanotube films. *Nano Lett* 8:982–987. <https://doi.org/10.1021/nl071945i>
- Murakami TN, Ito S, Wang Q, Nazeeruddin MK, Bessho T, Cesar I, Liska P, Humphry-Baker R, Comte P, Pechy P, Grätzel M (2006) Highly efficient dye-sensitized solar cells based on carbonblack counter electrodes. *J Electrochem Soc* 153A:2255–2261. <https://doi.org/10.1149/1.2200287>
- Shibata Y, Kato T, Kado T, Shiratuchi R, Takashima W, Kaneto K, Hayase S (2003) Quasi-solid dye sensitised solar cells filled with ionic liquid-increase in efficiencies by specific interaction between conductive polymers and gelators. *Chem Commun* 21:2730–2731. <https://doi.org/10.1039/b305368g>
- Saito Y, Kubo W, Kitamura T, Wada Y, Yanagida S (2004) I–/I₃– redox reaction behavior on poly(3,4-ethylenedioxythiophene) counter electrode in dye-sensitized solar cells. *J Photochem Photobiol A* 164:153–157. <https://doi.org/10.1016/j.jphotochem.2003.11.017>
- Pringle JM, Armel V, MacFarlane DR (2010) Electrodeposited PEDOT-on-plastic cathodes for dye-sensitized solar cells. *Chem Commun* 46:5367–5369. <https://doi.org/10.1039/c0cc01400a>
- Li QG, Wu JH, Tang QW, Lan Z, Li PJ, Lin JM, Fan LQ (2008) Application of microporous polyaniline counter electrode for dye-sensitized solar cells. *Electrochem Commun* 10:1299–1302. <https://doi.org/10.1016/j.elecom.2008.06.029>
- Kim H, Veerappan G, Park JH (2014) Conducting polymer coated non-woven graphite fiber film for dye sensitized solar cells: superior Pt- and FTO-free counter electrodes. *Electrochim Acta* 137:164–168. <https://doi.org/10.1016/j.electacta.2014.06.012>
- Yue G, Wu J, Xiao Y, Huang M, Lin J, Lin JY (2013) High performance platinumfree counter electrode of molybdenum sulfide-carbon used in dye-sensitized solar cells. *J Mater Chem A* 1:1495–1501. <https://doi.org/10.1039/C9TA06887B>
- Veerender P, Saxena V, Jha P, Koiry SP, Gusain A, Samanta S, Gupta SK (2012) Free-standing polypyrrole films as substrate-free and Pt-free counter electrodes for quasi-solid dye-sensitized solar cells. *Org Electron* 13(12):3032–3039. <https://doi.org/10.1016/j.orgel.2012.08.039>
- Karahan İH, Tiltıl F (2016) Electrodeposition and corrosive properties of environmental ZnFe/polyaniline on low carbon steel. *Acta Phys Pol* 130:282–285. <https://doi.org/10.12693/APhysPolA.130.282>
- Ha YH, Nikolov N, Pollack SK, Mastrangelo J, Martin BD, Shashidhar R (2004) Towards a transparent, highly conductive poly(3,4-ethylenedioxythiophene). *Adv Funct Mater* 14(6):615–622. <https://doi.org/10.1002/adfm.200305059>
- Hamdani K, Adnane M, Sam S, Chaumont D, Belhousse S, Tighilt FZ, Lasmi K, Hamrani A (2019) Deep insight into electron transport and photovoltaic parameters in DSSCs. *Emerg Mater Res* 8:113–122. <https://doi.org/10.1680/jemmr.18.00088>
- Ali A, Jamal R, Shao W, Rahman A, Osman Y, Abdiryim T (2013) Structure and properties of solid-state synthesized poly(3,4-propylenedioxythiophene)/nano-ZnO composite. *Pro Nat Sci Mater* 23:524–531. <https://doi.org/10.1016/j.pnsc.2013.11.002>
- Guler FG, Sarac AS (2011) Electrochemical synthesis of poly[3,4-propylenedioxythiophene-co-N-phenylsulfonylpyrrole]: morphological, electrochemical and spectroscopic characterization. *Express Polym Lett* 5:493–505. <https://doi.org/10.3144/expresspolymlett.2011.48>
- Wei TC, Wan CC, Wang YY, Chen CC, Shiu HS (2007) Immobilization of poly(N-vinyl-2-pyrrolidone)-capped platinum nanoclusters on indium-tin oxide glass and its application in dye-sensitized solar cells. *J Phys Chem C* 111:4847–4853. <https://doi.org/10.1021/jp067501c>
- Yan X, Cui X, Li B, Li LS (2010) Large, solution-processable graphene quantum dots as light bsorbers for photovoltaics. *Nano Lett* 10:1869–1873. <https://doi.org/10.1021/nl101060h>

Publisher's Note Springer Nature remains neutral with regard to jurisdictional claims in published maps and institutional affiliations.